

Atmospheric circulation and storm events in the Black Sea and Caspian Sea

Research Article

Galina V. Surkova^{1*}, Victor S. Arkhipkin², Alexander V. Kislov¹

¹ Department of Meteorology and Climatology, Faculty of Geography, Lomonosov Moscow State University

² Department of Oceanology, Faculty of Geography, Lomonosov Moscow State University

Received 03 August 2013; accepted 08 October 2013

Abstract: Extreme sea storms are dangerous and a potential source of damage. In this study, we examine storm events in the Black Sea and Caspian Sea, the atmosphere circulation patterns associated with the sea storm events, and their changes in the present (1961-2000) and future (2046-2065) climates. A calendar of storms for the present climate is derived from results of wave model SWAN (Simulating WAves Nearshore) experiments. On the basis of this calendar, a catalog of atmospheric sea level pressure (SLP) fields was prepared from the NCEP/NCAR reanalysis dataset for 1961-2000. The SLP fields were subjected to a pattern recognition algorithm which employed empirical orthogonal decomposition followed by cluster analysis. The NCEP/NCAR reanalysis data is used to evaluate the occurring circulation types (CTs) within the ECHAM5-MPI/OM Atmosphere and Ocean Global Circulation Model (AOGCM) for the period 1961-2000. Our analysis shows that the ECHAM5-MPI/OM model is capable of reproducing circulation patterns for the storm events. The occurrence of present and future ECHAM5-MPI/OM CTs is investigated. It is shown that storm CTs are expected to occur noticeably less frequently in the middle of the 21st century.

Keywords: classification • atmospheric circulation • future climate • storm events

© Versita sp. z o.o.

1. Introduction

Many social and economic activities are affected by the variability of sea storms and extreme events. It is well known that the formation and variability of storm waves are strongly influenced by atmospheric circulation patterns.

Climate projection of weather hazards needs their classification. Classifications in meteorology and climatology have previously been used mainly in weather

forecasting [1]. In recent decades, especially after the advance of computers, the use of classifications has widened. Computer techniques made it possible to develop and routinely apply objective methods based on processing large amounts of data. There are two fundamental approaches to investigate the link between large-scale circulation and environmental variables [2–4]. The first one is known as the circulation-to-environment approach [3] and groups the circulation data of interest (e.g. sea level pressure, geopotential height, etc.) into circulation types (CTs) according to a selected methodology (clustering, principal component analysis (PCA), regression, etc.). This highlights relationships between CTs and the local-scale environmental variable

*E-mail: galina.surkova@mail.ru

(e.g. storm waves). In contrast, the environment-to-circulation approach is based on classification of the circulation data for certain criteria of environmental variable, so that composite maps of the circulation variable can be derived for a specific environmental condition. Both approaches are widely used in various fields of the atmospheric sciences. The circulation-to-environment approach was successfully implemented in the COST733 project (<http://cost733.met.no>) entitled "The harmonization and application of weather types classifications for European regions". An extensive review of existing classification methods and those used in COST733 can be found in Huth *et al.* [1]. Investigation based on the environment-to-circulation approach is used for surface ozone concentration in Central Europe and is discussed in Demuzere *et al.* [3]. Numerous studies present the results of various regional classifications e.g., [5–8].

In this study we use the environment-to-circulation approach for storm events in the Black Sea and Caspian Sea. The Black Sea (together with the Sea of Azov) is located in south-eastern Europe and is the most isolated part of the World Ocean (Figure 1). Because of the wind activity over the sea, heavy waves develop mostly in the autumn and winter [9]. Depending on the wind speed direction, waves with heights of 1–3 m dominate. In regions of open sea, the wave height may reach 7 m, and during strong storms it may be even higher. The southwestern and southeastern parts of the sea are the calmest; in these regions, strong winds are rare and wave heights do not usually exceed 3 m even during storms.

The Caspian Sea forms the largest enclosed basin on the planet (Figure 1). Storm waves generally develop in the winter and spring from northerly winds. Strong long-term storms are most characteristic of the open areas of the Middle Caspian, where the winds (?) are mostly from the northwest and southeast [10]. Depending on the wind direction storms are observed in different parts of the sea. The largest storm waves are observed around the Apsheron Archipelago during northerly storms in the wintertime, where wave height may reach 8 and even 9–10 m during extreme events. Under southeasterly winds, the largest waves develop in the north of the Middle Caspian, in the Makhachkala-Derbent region and off the Mangyshlak Peninsula, where there is a 5% probability that waves will reach 6–7 m. A similar wave height is observed in the open part of the sea at southeasterly storms. Even the strongest easterly winds induce waves that are smaller than 2–3 m. In the North Caspian, wind wave development is restricted by the small sea depths in the region. The wind-wave regimes of the Black and Caspian Seas are poorly studied because there are no regular instrumental observations of waves in the

open parts of the seas. The principal characteristics of the waves have been determined using calculations; this is also true of the wave heights cited above. Our investigation addresses this sparsity of data by using the numerical wave model SWAN (Simulating WAves Nearshore) to calculate storm statistics. Storm days are based on a wave height of 4 m or more. For these days, sea level pressure (SLP) fields are used to classify circulation types.

The goals of this paper are to: 1) improve our understanding of storm variability in the Southern Russian seas by investigating the atmospheric circulation during these events as defined by classification of circulation types, and 2) to prepare the climate projection of these events. Details of the atmospheric circulation accompanying and forcing a sea storm is very complicated and even non-hydrostatic, meso-scale weather forecast models are not always capable of correctly simulating the wind field during sea storm. However, statistical analysis of long-term observations combined with climate model projections allows the probability of future storms to be calculated.

2. Data

2.1. Storm calendar

A calendar of storm events was derived for the period 1948 – 2010 for this study. The numerical storm simulator SWAN (Simulating WAves Nearshore) was used, a third-generation wave model that was developed at Delft University of Technology. It computes random, short-crested wind-generated waves in coastal regions and inland waters [11, 12]. The model is based on the wave action balance equation (or energy balance in the absence of currents), with sources and sinks. It uses typical formulations for wave growth by wind, wave dissipation by white-capping, and four-wave nonlinear interactions (quadruplets or "quads"). SWAN includes wave propagation processes comprising propagation through geographic space, refraction and shoaling due to spatial variations in bottom and current, diffraction, blocking and reflections by opposing currents and transmission through, blockage by or reflection against obstacles. It also includes processes describing wave generation and dissipation including the following: generation by wind, dissipation by white-capping, dissipation by depth-induced wave breaking, dissipation by bottom friction and wave-wave interactions in both deep and shallow water. Wind forcing data was extracted from NCEP/NCAR reanalysis [13] at the 6-hourly intervals available (0000 UTC, 0600 UTC, 1200 UTC and 1800 UTC). The spatial

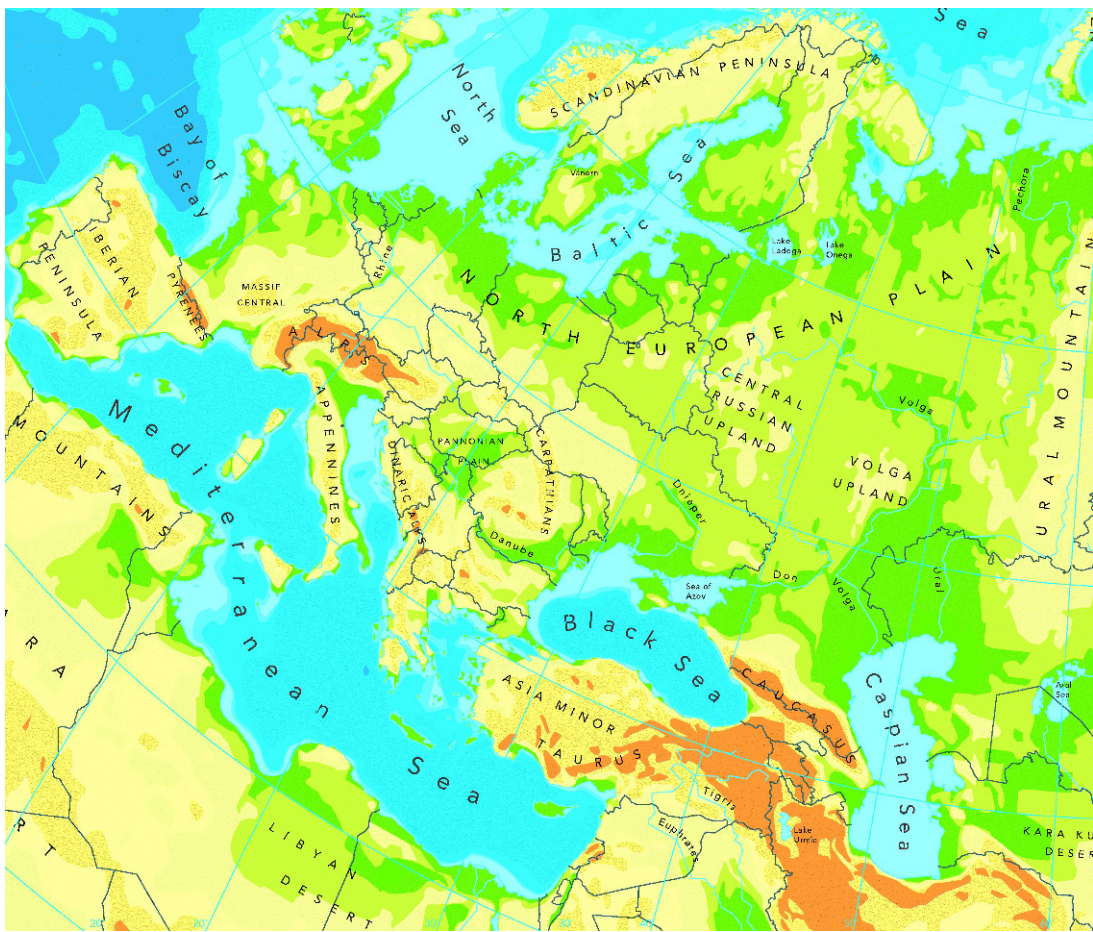


Figure 1. Europe, Black Sea and Caspian Sea location (permitted free of charge by <http://www.eea.europa.eu/legal/copyright>).

resolution of the SWAN numerical grid was about 5 km. An overview of numerical simulations is described in [14]. For our study, days were chosen when modeled wave height was 4 m or more. The threshold of 4 m is based on the state standard for safety in emergencies [15], which specifies waves of 4 m or more in the coastal zone and 6 m or more in the open sea as hazardous. 137 cases were identified for the Black Sea and 94 for the Caspian Sea between 1948 and 2010. In this paper, days from this calendar will be referred to as storm days or SWAN storm days. Other examples of SWAN implementations for the Russian southern seas are discussed in [16–21].

2.2. Climate projection

For the climate projection of storm events we used daily SLP fields (0–90°E, 30–80°N) generated by the coupled

AOGCM of Max Plank Institute ECHAM5/MPI-OM at T63L31 resolution [22] within the framework of CMIP3 project [23].

ECHAM5/MPI-OM consists of models for the atmosphere (ECHAM5) and the ocean (MPI-OM). In the atmospheric model [22, 24], vorticity, divergence, temperature and the logarithm of surface pressure are represented by a truncated series of spherical harmonics (triangular truncation at T63). The advection of water vapour, cloud liquid water and cloud ice is treated by a flux-form semi-Lagrangian scheme. A hybrid sigma/pressure system is used in the vertical direction (31 layers with the top model level at 10 hPa). The model uses state-of-the-art parameterizations for short-wave and long-wave radiation, stratiform clouds, cumulus convection, boundary layer and land surface processes, and gravity wave drag.

The ocean model MPI-OM [25] uses the primitive

equations for a hydrostatic Boussinesq fluid with a free surface. It is discretized into 40 vertical layers, and the bottom topography is resolved by means of partial grid cells. The ocean has a nominal (spatial?) resolution of 1.5° and the poles of the curvilinear grid are shifted to land areas over Greenland and Antarctica. Concentration and thickness of sea ice are calculated by means of a dynamic and thermodynamic sea ice model.

In the coupled model [26], the ocean model passes the sea surface temperature, sea ice concentration, sea ice thickness, snow depth on ice, and ocean surface velocities to the atmospheric model. The atmospheric model runs with these boundary conditions for one coupling time step (one day) and accumulates the forcing fluxes. These fluxes are then transferred to the ocean model. The model does not employ flux adjustments.

Global ECHAM5-MPI/OM SLP datasets were taken from the open-source CMIP3 archive at the Program for Climate Model Diagnosis and Intercomparison (PCMDI) [<http://www-pcmdi.llnl.gov>], for the, for 1960–2000 (climate of the 20th Century experiment, 20C3M) and 2046–2065 (SRES, emission scenario A2 [27]).

As shown in [28], ECHAM5-MPI/OM appears to closely reproduce daily mean SLPs and the frequencies in circulation types, especially for the late autumn, winter and early spring periods. This justifies the use of the model because the majority of the storm activity in the Black and Caspian Seas is observed in the cold season [29, 30].

2.3. Reanalysis data

To determine daily circulation patterns at a regional scale, daily mean sea level pressure (MSLP) data was used from the NCEP/NCAR reanalysis dataset [13] on a $2.5^\circ \times 2.5^\circ$ grid for the European and Western Russia Region (0 – 90° E, 30 – 80° N). The data is obtained for the period 1948–2011.

3. Methods

Our approach of atmospheric circulation classification for storm events relies on the understanding that storm waves are mainly the product of wind speed and direction, which determine the value of the flux of momentum from the atmosphere to the sea. Storm wave parameters also greatly depend on the sea size, its depth, bottom relief, coastline configuration etc. But these factors are not results of atmospheric processes on as short a time-scale as one storm. It is the surface wind that plays the most important role in individual storm forcing. Furthermore, the wind depends on the atmospheric

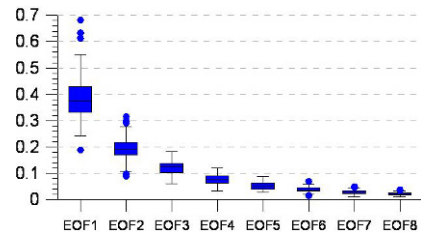


Figure 2. Contribution of EOF modes to daily SLP variability.

pressure field configuration and the value of the horizontal pressure gradient. Fortunately, the pressure is the most reliable meteorological parameter reproduced by reanalyses and by climate general circulation models, and so a straightforward expansion of the study to model data is possible. MSLP has already been used successfully in previous classification procedures, e.g. [1, 6, 8].

The goals of our study were the following: to classify SLP grids accompanying storm events (from now on referred to as storm SLP); to extract the main features of circulation patterns for every type; to evaluate the frequency of every type for the modern climate and possible changes in frequency in the future.

There are a lot of different ways to describe atmospheric circulation, and this variety is reflected in the number of different sorts of circulation-based classifications. For one of the most detailed descriptions of them we refer to [1]. In our study, circulation types are obtained by cluster analysis (k –means approach, e.g., [31]) preprocessed by Empirical Orthogonal Function (EOF) analysis, e.g., [32] to reveal few leading modes determining the most part of variance. These techniques of EOF decomposition and k –means cluster analysis, together or in combination with other techniques, are widely used in circulation type classifications, e.g., [2, 7, 8, 33–36].

For this study, firstly a dataset consisting of 30 daily SLP grids was prepared for every storm from the calendar, including 15 days before and 15 days after each storm day. After EOF decomposition of daily SLP grids, the first three eigenvectors were retained, describing more than 70% of the variability (Figure 2). Therefore, high-frequency perturbations were filtered out. Henceforth they are referred to as SLP_{EOF} .

SLP_{EOF} fields for storm days (according to the storm calendar of the sea) were used as input variables to classify circulation patterns. Definition of circulation types was carried out using the k –means cluster analysis. The k –means algorithm starts with a preset number of clusters k and then moves objects between clusters with

the goal of, first, minimizing the variance within clusters and, second, maximizing the variance between clusters. In this study, cluster centroids (ensemble mean of cluster members) were constructed for each circulation type by averaging the SLP grids of all days that belonged to the same circulation type. The dependence of the assigned SLP field on the sea size was checked for certain (all?each cluster?) clusters: we started from an initial area covering 0-90E, 30-80N, and reduced it gradually until it was comparable with the sea size. It only had a very minor influence on the results. Therefore, we left the area at 0-90°E, 30-80°N for centroids construction to gain a full, large-scale synoptic view of the circulation pattern.

For the next step, daily SLP data of EHCAM5-MPI/OM model for the period 1960-2000 was sorted based on (?) previously derived circulation patterns. As one of distance measures [1, 37, 38], space correlation was used between model data and reanalysis SLP fields for days from the storm calendar. To eliminate 'noise' on the boundaries of the rather large initial domain (0-90E, 30-80N) but to save individual features of the SLP field, correlation was estimated for 25-50E, 35-65N for the Black Sea, 30-70E, 30-70N for the Caspian Sea. The spatial scale of the smaller domains is comparable with size of such typical mid-latitude synoptic structures as cyclones and anticyclones governing surface winds and therefore storm waves. Since cluster analysis allowed assigning every case from this calendar to the respective circulation type, a model day when EHCAM5-MPI/OM data was highly correlated with the NCEP/NCAR field for the storm case was rated as a model day with the same CT.

The same procedure was also applied to the model data for the period 2046-2065, i.e. the correlation was calculated between daily model SLP and reanalysis SLP fields from the storm calendar. Before this correlation procedure, the model data were interpolated on the reanalysis grid. If the daily SLP field had a correlation coefficient higher than a threshold value, it was assigned to the same CT as the reference reanalysis SLP field from the storm calendar. The threshold for the correlation coefficient r was chosen separately for each sea on the basis of the best agreement of the number of storm cases simulated by ECHAM5-MPI/OM and by SWAN. Usually r was satisfactory when equal to 0.95-0.98.

4. Results and discussion

4.1. Black Sea

Within the variety of the atmospheric circulation governing the climate of the Black Sea, there are two main types of sea level pressure field derived by cluster analysis and

associated with SWAN storm days (Figure 3).

For the first circulation type CT 1 (57% of events), the trough moves to the Black Sea from the eastern Mediterranean Sea in Anatolia, Western Asia, and often forms an independent local cyclone over the Black Sea. If the centre of the cyclone is located over the southern part of the Black Sea or over Asia Minor, prevailing winds are NE, E and SE. When the horizontal size of the cyclone is comparable with the sea size, the wind directions over the sea are rather complex. At the same time, a vast anticyclone overspreads European Russia and Western Siberia blocking northward movement of the southern cyclone. The second type CT 2 (the other 43% of events) is characterized by a low pressure centre over the northern seas (Barentz or Norwegian). The leading edge of the trough (usually observed in the middle and upper troposphere as well as near the surface) develops quickly and trails southeast rapidly from a northern low-pressure center. When this cold air reaches the Black Sea in winter, a local cyclone may be generated.

These two circulation types are the most effective for the formation of storms. The configuration of the pressure field is such that the high wind flow has the largest distance over the open sea to accelerate and to induce storm waves. In these cases storms cover a large part of the sea. More local storms occur with southern or northern winds or when a fairly small cyclone forms over the sea. This can occur for a CT 1 or CT 2 depending on the source of the instability - a northern or southwestern trough. Storms initiated by these Black Sea cyclones can also be very cruel.

Both observations and modeling in previous studies, e.g., [29, 39, 40] agree that the number of storm events in the Black Sea does not increase by the end of the twentieth century and may even reduce. The same tendency is seen in SWAN results (Figure 4). Analysis of CT frequency shows that the proportion of the two CTs is redistributed slightly between the periods 1961-1980 and 1981-2000, with the frequency of CT 1 events becoming higher than CT 2 in the latter period.

Storms in the Black Sea occur mainly in November-March [9], as is clearly seen from the frequency of storm days revealed by SWAN results (Figure 5). EHACM5-MPI/OM data for storm SLP (SLPEHACM5) are in agreement with the SWAN storm results (Figure 5). Because of some overestimation in the beginning of the year and underestimation in the end, the peak of storm activity is shifted one month later in ECHAM5-MPI/OM compared to the SWAN results. Summer time is quite calm, although some days where storms occurred were reproduced by SWAN (which is in agreement with observations [29]). EHACM5-MPI/OM does not show the occurrence of storms in the summer, and [28] shows that

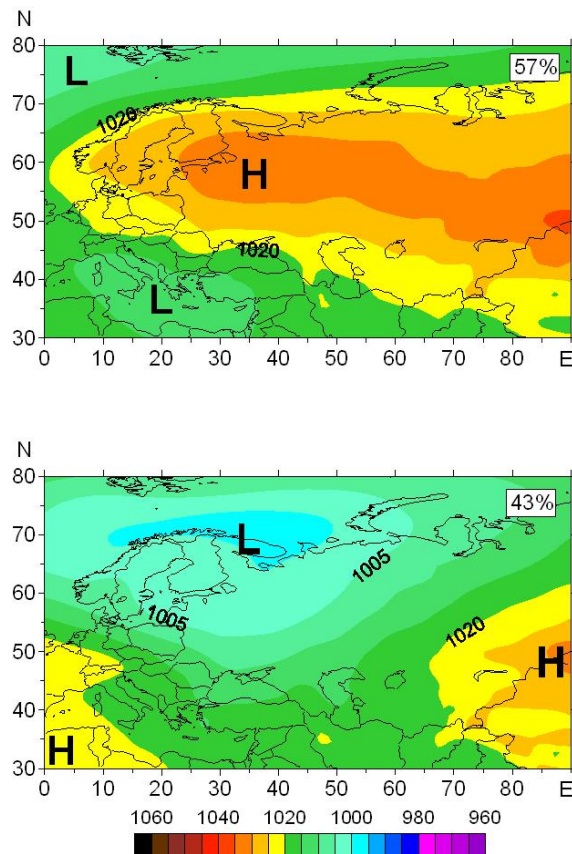


Figure 3. Centroids (ensemble means) of two clusters for SLP_{EOF} .

circulation frequencies, especially for the late autumn, winter and early spring periods are reproduced much better by EHAM5 than for the warm season.

When comparing SLP fields of EHAM5-MPI/OM and NCEP/NCAR for 1961–2000, two thresholds were chosen for the correlation coefficient: $r \geq 0.95$ and $r \geq 0.98$. Previous investigation [39] showed that $r \geq 0.95$ is enough for EHAM5-MPI/OM and reanalysis results to have good agreement in the number of days with wind speed of 15 m/s and more, which is considered to be the threshold for storm-wave development in the Black Sea and Caspian Sea [9, 10, 29, 30]. The second value $r \geq 0.98$ is chosen because with this correlation the number of storm days reproduced by EHAM5-MPI/OM is the same as that given by the SWAN model. The latter r is therefore the preferred one. However, the threshold for storm wave height is fixed at $H = 4$ m, and days with H slightly less than 4 m were not taken into account.

As Figure 6 and Figure 7 show, EHAM5-MPI/OM

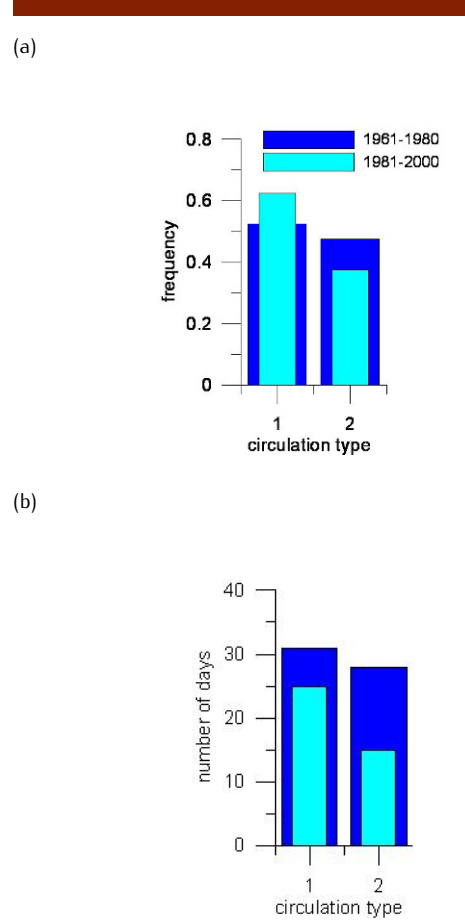


Figure 4. Relative (a) and absolute (b) frequency of storm days with wave height $H \geq 4$ m from SWAN results.

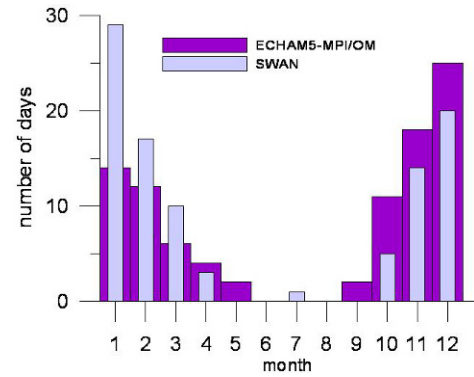
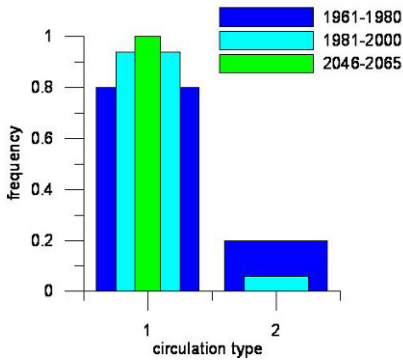


Figure 5. The annual pattern of SWAN storm frequencies (with wave height ≥ 4 m) and EHAM5-MPI/OM results of storm SLP ($r \geq 0.98$), mean values for 1961–2000.

(a)



(b)

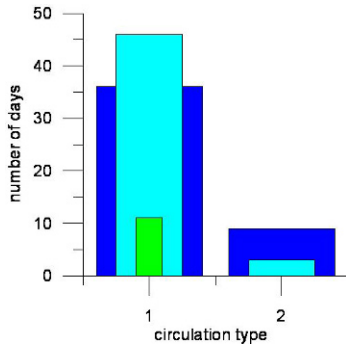


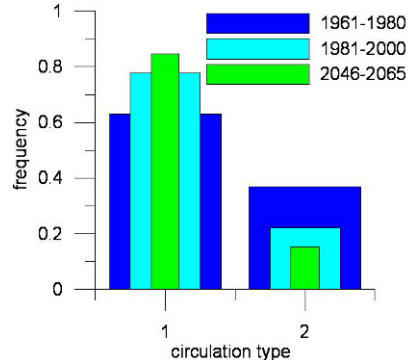
Figure 6. Relative (a) and absolute (b) frequency of storm days from EHCAM5-MPI/OM data, $r \geq 0.98$.

captures the main features of the circulation type ratio and its changes between 1961–1980 and 1981–2000 for the present climate. The role of the second CT is underestimated for both periods, but nevertheless the trend is reproduced, and the whole number of storm SLP cases is close to the SWAN results.

To analyze possible changes in storm SLP frequency in the future, we used ECHAM5 results from modeling the A2 SRES emission scenario [27], the most negative variant of human impact to the climate including high greenhouse gas emissions, non-effective land use, fast population growth etc. SRES A2 scenario has the highest temperature increase by the end of the 21st century, about 3.5°C [41]. According to the ECHAM5-MPI/OM results, projected mean global temperature will increase by about 1.5°C by 2050 and by 4°C by 2100 relative to 1980–1999 [41].

Figure 6 and Figure 7 show that storm activity in the

(a)



(b)

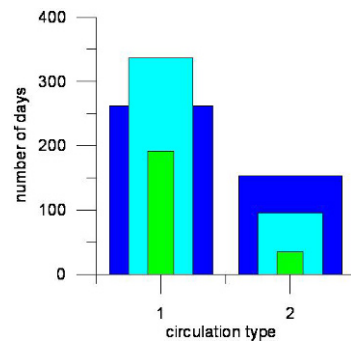


Figure 7. Relative (a) and absolute (b) frequency of storm days from EHCAM5-MPI/OM data, $r \geq 0.95$.

Black Sea will be strongly reduced by the middle of the 21st century, and so the tendency of the previous decades will continue. If mid-latitude cyclone storm tracks move northwards. According to an IPCC report [39], the multi-model ensemble mean SLP projection shows SLP increase over the Mediterranean Sea and Black Sea, especially between December and February. This may explain why storm activity is projected to weaken in our results.

4.2. Caspian Sea

There are several classifications of storm synoptic situations for the Caspian Sea. All of them are based on careful visual analysis of daily SLP from (?) AT500 and other maps. There are three dominating synoptic situations generating storms in this sea, as described in the most comprehensive handbook on the Caspian Sea which integrates all previous studies of the Caspian [30].

Two of the situations are connected with anticyclone ridges from Azor maximum or from the northern seas. The third one, characterized by high cyclonic activity over the sea, is not observed as often and results in local storms. Three circulation types resulted from cluster analysis and were associated with SWAN storm days as shown in Figure 8. The first and second types are in good agreement with the results of the subjective methods described above and illustrate the influence of anticyclonic ridges from the north and from Azor maximum. The third CT reflects the role of Caspian cyclones.

The frequency of different circulation types differs noticeably between 1961-1980 and 1981-2000 (Figure 9). The frequency of the first type decreases by the end of the 20th century when the proportions of CT 2 and CT 3 grow. This may be caused by the observed warming of central Russia, reduction of Arctic cold waves and changes in the pressure field, corresponding to a negative tendency over European Russia and Western Siberia and a positive trend over most of Europe, the Black Sea and Caspian Sea, especially in winter time [41].

Reproducing annual patterns of storm SLP occurrence, ECHAM5-MPI/OM model is less accurate for the Caspian Sea than for the Black Sea (Figure 10). Nevertheless it realistically reflects the overwhelming majority of storm processes in the cold season (November-March). This fact may justify further analysis. Winter storms dominate because of the increase in cyclonic activity. For example, strong winds exciting storm waves occur on the periphery of winter Asian anticyclones or the Azor maximum ridge. Observations and reanalysis ERA-40 show atmospheric pressure grow in both areas in 1979-2001, resulting in increasing anticyclonic influence over the Caspian [41].

The second circulation type prevailing in ECHAM5-MPI/OM results (Figure 11) is more dominant than in SWAN data. Despite discrepancies, the model results show a slight decrease of storm SLP events from 30 cases in 1961-1980 to 28 cases in 1981-2000.

Changes in circulation types for the projected climate of 2046-2065 are not as noticeable as for the Black Sea (Figure 10). They could be characterized as a return to the regime of 1961-1980, involving an increase in CT 2 occurrences and a decrease in CT 1 occurrences. The lack of the third circulation type in projected SLP fields can be explained by the results of climate modeling mentioned above [41], where a pressure increase is expected over the Caspian sea and surroundings.

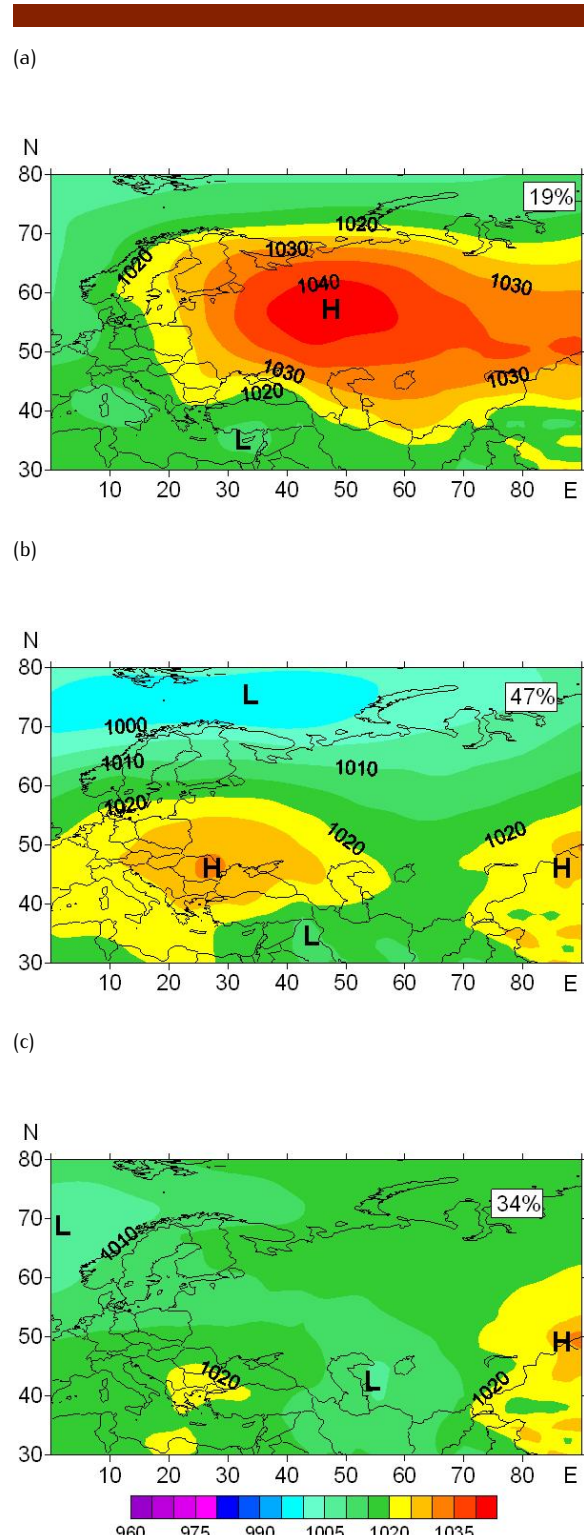
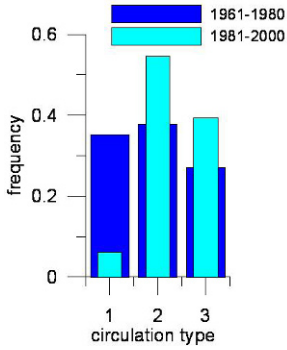


Figure 8. Centroids (ensemble means) of four clusters for an ensemble forecast for hemispheric 500-mb height at a lead time of eight days.

(a)



(b)

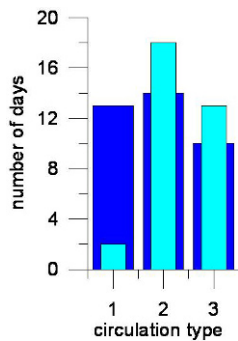
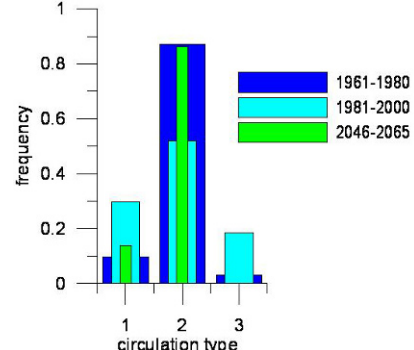


Figure 9. Relative (a) and absolute (b) frequency of storm days with wave height $H \geq 4$ m, SWAN results.

(a)



(b)

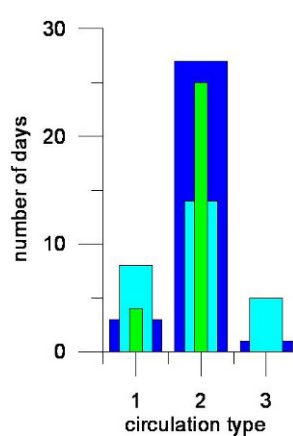


Figure 11. Relative (a) and absolute (b) frequency of storm days from EHCAM5-MPI/OM data, $r \geq 0.95$.

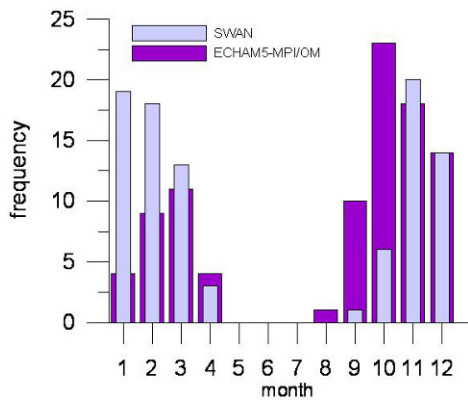


Figure 10. The annual pattern of SWAN storm frequencies (with wave height ≥ 4 m) and ECHAM5-MPI/OM results of storm SLP ($r \geq 0.94$), mean values for 1961–2000.

5. Conclusion

This is the first study of the Black and Caspian Seas where atmospheric circulation pattern classification derived through statistical analysis of SLP fields is developed for storm events. The occurrence of circulation types is investigated for the present climate on the basis of NCEP/NCAR reanalysis and wave model SWAN modeling. It is shown, in agreement with previous studies, that by the end of the 20th century the storm activity had decreased in both the Black and Caspian Seas. It was found that the frequency of circulation types was redistributed in 1981–2000 compared to 1961–1980. The circulation types for a 40-year control run (1961–2000) of the ECHAM5-MPI/OM CGCM for the Black Sea and Caspian Sea are evaluated using the

NCEP/NCAR reanalysis database. In general, ECHAM5-MPI/OM appears to be able to reproduce the main features in frequencies of circulation types although there are some differences with SWAN results. Analysis of potential future changes of circulation patterns is carried out for ECHAM5-MPI/OM climate scenario A2. Both for the Black and Caspian Seas, a noticeable decrease of storm SLP frequency is expected. The approach suggested here could provide a rather simple methodology to detect changes and differences in circulation patterns for hazardous weather phenomena. It could also be used as an appropriate tool for CGCM evaluation.

Acknowledgements

The research was carried out with the financial support of the "Risk assessment of ocean related extreme events in the coastal zone" project (no. 11.G.34.31.0007).

References

[1] Huth R., Beck C., Philipp A., Demuzere M., Ustrnul Z., Cahynov M.'Kysel'y J., Tveito O. E. Classifications of Atmospheric Circulation Patterns Recent Advances and Applications, *Trends and Directions in Climate Research: Ann. N.Y. Acad. Sci.* 1146, 2008, 105-152. doi: 10.1196/annals.1446.019.

[2] Cannon A.J., Whitfield P.H., Lord E.R., Synoptic map pattern classification using recursive partitioning and principal component analysis, *Monthly Weather Review* 130, 2002, 1187-1206

[3] Demuzere M., Kassomenos P., Philipp A., The COST733 circulation type classification software: an example for surface ozone concentrations in Central Europe, *Theor Appl Climatol.* 105, 2011, 143-166, doi 10.1007/s00704-010-0378-4

[4] Yarnal B., Synoptic climatology in environmental analysis. Belhaven Press, London, 1993

[5] Brisson E., Demuzere M., Kwakernaak B., Van Lipzig N. P. M., Relations between atmospheric circulation and precipitation in Belgium, *Meteorol Atmos Phys.*, 2010, doi 10.1007/s00703-010-0103-y

[6] Corte-Real J., Qian B., Xu H., Regional climate change in Portugal: precipitation variability associated with large-scale atmospheric circulation, *International Journal of Climatology* 18, 1998, 619-635

[7] Corte-Real J., B. Qian & H. Xu, Circulation patterns, daily precipitation in Portugal and implications for climate change simulated by the second Hadley Centre GCM, *Clim. Dyn.* 15, 1999, 921-935

[8] Santos J. A., Corte-Real J., Leite S.M., Weather regimes and their connection to the winter rainfall in Portugal, *Int. J. Climatol.* 25, 2005, 33-50

[9] Kostianoy A., Kosarev A. (Eds.). The Black Sea Environment. The Handbook of Environmental Chemistry, vol.5, part Q, Springer, 2008, 459, doi 10.1007/978-3-540-74292-0

[10] Kostianoy A., Kosarev A. (Eds.). The Caspian Sea Environment. The Handbook of Environmental Chemistry, vol.5, part P, Springer, 2005, doi 10.1007/b138238

[11] Booij, N., R. C. Ris, and L. H. Holthuijsen: A third-generation wave model for coastal regions. 1. Model description and validation, *J. Geophys. Res.* 104, 1999, 7649-7666

[12] SWAN. Scientific and technical documentation. SWAN Cycle III. Version 40.91A. [Available from Delft University of Technology, Faculty of Civil Engineering and Geosciences, Environmental Fluid Mechanics Section, P.O. Box 5048, 2600 GA Delft, The Netherlands; <http://www.swan.tudelft.nl>]

[13] Kalnay *et al.*, The NCEP/NCAR 40-year reanalysis project. *Bull. Amer. Meteor. Soc.* 1996, vol.77, 437-470

[14] Arkhipkin V., Dobroliubov S., Long-term variability of extreme waves in the Caspian, Black, Azov and Baltic Seas, *Geophysical Research Abstracts*, Austria, Vienna, 2013, vol. 15, EGU2013-7484

[15] Bezopasnost v chrezvychajnyh situatsijah. Monitoring i prognozirovanie opasnyh hydrologicheskikh javlenij i processov [Safety in emergencies. Monitoring and forecasting of dangerous hydrological phenomena and processes. General requirements. State standard.] GOST R 22.1.08-99. 1999 (in Russian)

[16] Akpinar A., van Vledder G.P., Komurcu M.I., Ozger M., Evaluation of the numerical wave model (SWAN) for wave simulation in the Black Sea. *Continental Shelf Research*, Volumes 50-51, 15 December, 2012, 80-99

[17] Hadadpour S., Moshfeghi H., Jabbari E., Kamranzad B., Wave hindcasting in Anzali, Caspian Sea: a hybrid approach. In: Conley D.C., Masselink G., Russell P. E., O'Hare T. J. (eds.), *Proceedings 12th International Coastal Symposium (Plymouth, England)*, *Journal of Coastal Research*, Special Issue 65, 2013, 237 - 242

[18] Rusu E., Rusu L., Soares C. G., Prediction of Extreme Wave Conditions in the Black Sea with Numerical Models. In proceeding of: 9th International Workshop on Wave Hindcasting and Forecasting, At Victoria, Canada, 2006

[19] Strukov B. S., Zelenko A. A., Resnyansky Yu. D.,

Martynov S. L., A System of Wind Wave Forecasting in the World Ocean and Seas of Russia. The System's Structure and its Main Constituents. In: WGNE Blue book, Section 8, Development of and advances in ocean modelling and data assimilation, sea-ice modelling, wave modeling, 2012, 3-4

[20] Strukov B .S., Zelenko A. A., Resnyansky Yu. D., Martynov S. L., Verification of the Wind Wave Forecasting System for the Black, Azov and Caspian Seas. In: WGNE Blue book, Section 8, Development of and advances in ocean modelling and data assimilation, sea-ice modelling, wave modeling, 2012, 5-6

[21] Buhanovslij A. V., Lopatukhin L. I., Chernysheva E. S., Kolesov A. M. Storm na Chernom more 11 nojabrja 2007 i statistika ekstremalnyh stormov morja (The storm on the Black Sea, November 11, 2011, and extreme storm statistics for the sea). *Izvestia RGO*, 2009, V.141 (2). 71-79. (in Russian)

[22] Roeckner E., Baum G., Bonaventura L., Brokopf R., Esch M., Giorgetta M., Hagemann S., Kirchner I., Kornblueh L., Manzini E., Rhodin A., Schlese U., Schulzweida U., Tompkins A., The atmospheric general circulation model ECHAM5. Report No. 349. Max-Planck-Institut für Meteorologie, Hamburg, November 2003, 140 p. [Available from Max Planck Institute for Meteorology, Bundesstr. 53, 20146, Hamburg, Germany]

[23] Meehl G. A., Covey C., Delworth T., Latif M., McAvaney B., Mitchell J. F. B., Stouffer R. J., Taylor K. E., The WCRP CMIP3 multimodel Dataset: a new era in climate change research, *Bull. Amer. Met. Soc.* 88, 2007, 1383-1394, doi:10.1175/BAMS-88-9-1383.

[24] Roeckner E., Brokopf R., Esch M., Giorgetta M., Hagemann S., Kornblueh L., Manzini E., Schlese U., Schulzweida U., Sensitivity of simulated climate to horizontal and vertical resolution in the ECHAM5 atmosphere model, *Journal of Climate* 19, 2006, 3771-3791

[25] Marsland S. J., Haak H., Jungclaus J. H., Latif M., Roske F., The Max-Planck-Institute global ocean/sea ice model with orthogonal curvilinear coordinates, *Ocean Modelling* 5, 2003, 91-127

[26] Jungclaus J. H., Botzet M., Haak H., Keenlyside N., Luo J-J., Latif M., Marotzke J., Mikolajewicz U., Roeckner E., Ocean circulation and tropical variability in the coupled model ECHAM5/MPI-OM, *Journal of Climate* 19, 2006, 3952-3972

[27] Nakicenovic N., Swart R. (Eds.), Special Report on Emissions Scenarios: A special report of Working Group III of the Intergovernmental Panel on Climate Change, Cambridge University Press, 2000, 599

[28] Demuzere M., Werner M., van Lipziga N. P. M., Roeckner E., An analysis of present and future ECHAM5 pressure fields using a classification of circulation patterns, *Int. J. Climatol.* 29, 2009, 1796-1810

[29] Terziev F. S. (Ed.) *Gidrometeorologija i gidrokhimija morey SSSR* [Hydrometeorology and hydrochemistry of the seas in the USSR]. Hydrometeoizdat, Leningrad, 1991, Vol.4-1, Chernoe more [Black Sea], *Gidrometeorologicheskie uslovia* [Hydrometeorological conditions], 430 p. (in Russian)

[30] Terziev F. S. (Ed.) *Gidrometeorologija i gidrokhimija morey SSSR* [Hydrometeorology and hydrochemistry of the seas in the USSR]. Hydrometeoizdat, Leningrad, 1992, Vol.6-1, Kaspijskoe more [Caspian Sea], *Gidrometeorologicheskie uslovia* [Hydrometeorological conditions], 360 p. (in Russian)

[31] Hartigan, J. A., Wong, M. A., Algorithm 136. A k-means clustering algorithm. *Applied Statistics*, 1978, 28, 100

[32] Preisendorfer R.W., Principal Component Analysis in Meteorology and Oceanography, Elsevier, 1988, 425

[33] Cassou C., Euro-Atlantic regimes and their teleconnections. Proceedings: ECMWF Seminar on Predictability in the European and Atlantic regions, 6-9 September 2010, 1-14, 2010

[34] Stahl, K., Moore R. D., McKendry I. G., The role of synoptic-scale circulation in the linkage between large-scale ocean-atmosphere indices and winter surface climate in British Columbia, Canada, *Int. J. Climatol.* 26, 2006, 541-560

[35] Philipp A., Bartholy J., Beck C., Erpicum M., Esteban P., Fettweis X., Huth R., James P., Jourdain S., Kreienkamp F., Krennert T., Lykoudis S., Michalides S. C., Pianko-Kluczynska K., Post P., Alvarez D. R., Schiemann R., Spekat A., Tymvios F. S., Cost733cat - a database of weather and circulation type classifications, *Phys Chem Earth* (Special Issue) 35, 2010, 360-373

[36] Solman S. A., Menendez C. G., Weather regimes in the South American sector and neighbouring oceans during winter, *Climate Dynamics* 21, 2003, 91-104

[37] Brinkmann W. A .R., Modification of a correlation-based circulation pattern classification to reduce within-type variability of temperature and precipitation, *Int. J. Climatol.* 20, 2000, 839-852

[38] Lund I. A., Map-pattern classification by statistical methods, *J. Appl. Meteorol.* 2, 1963, 56-65

[39] Surkova G. V., Kislov A. V., Koltermann P. K., Large-scale atmospheric circulation and extreme wind events during the Black sea storms. *Geophysical Research Abstracts*, 2012, vol. 14, EGU2012-4751

[40] Valchev N. N., Trifonova E. V., Andreeva N. K.,
Past and recent trends in the western Black Sea
storminess, *Nat. Hazards Earth Syst. Sci.* 12, 2012,
961-977, doi:10.5194/nhess-12-961-2012

[41] IPCC, 2007: Climate Change 2007: The Physical
Science Basis. Contribution of Working Group I to the
Fourth Assessment Report of the Intergovernmental

Panel on Climate Change [Solomon, S., D. Qin, M.
Manning, Z. Chen, M. Marquis, K. B. Averyt, M.
Tignor and H. L. Miller (eds.)], Cambridge University
Press, Cambridge, United Kingdom and New York,
NY, USA, 2007